J. Fluid Mech. (1969), *vol.* 38, *part* 4, *pp.* 657–671
Printed in Great Britain

Adiabatic transverse waves in a rotating fluid

By C. SOZOU AND J. SWITHENBANK
The University, Sheffield

(Received 30 December 1968)

Adiabatic disturbances propagating as transverse waves in an inviscid fluid rotating as a Rankine vortex about the axis of its cylindrical container are considered. The propagation of the first mode of the first two harmonic waves has been investigated. Relative to a fixed co-ordinate system, for each harmonic, there are three waves. Two waves are rotating in the same direction as the fluid, one faster and the other slower than the core of the fluid, and one wave rotates in the opposite direction. The latter is stable and relative to the core of the rotating fluid it is the fastest wave. Relative to the container, the other two waves are speeded up by rotation. However, relative to the rotating core, the angular velocity of the fast wave decreases when the fluid is speeded up, and when it is zero the wave breaks down. As the region of potential flow decreases the angular velocity of the slow wave increases and its amplitude decreases, and in the limit of vanishing potential flow, the wave rotates as fast as the fluid and its amplitude tends to zero.

1. Introduction

Rotating fluids, due to their importance in connexion with geophysical phenomena and engineering applications, have been studied by many authors. A survey of rotating fluids can be found in a recent paper by Lighthill (1966).

In many practical applications, such as combustion chambers of solid propellant rocket motors, the rotation of the fluid is associated with strong transverse waves which give rise to intense vortices. Such waves and vortices have been observed and reported by Swithenbank & Sotter (1964). When the cylindrical walls of the chamber are composed of burning propellant, the flow normal to the surface and the combustion process drive the waves with a wide band amplification (Cantrell & Hart 1964).

Several other experimental observations have been reported, and when flow is introduced tangentially at the periphery of a cylindrical chamber, and exhausted at an axial nozzle, a Rankine-type vortex is observed (Keyes 1960, Roschke & Pivirotto 1965). At diameters greater than that of the nozzle, conservation of angular momentum must cause the formation of a potential vortex, although in practice, due to viscous dissipation, the vortex is not quite potential. The tangential velocity attains a maximum value at a radius of between 0·5 and 0·9 of the nozzle radius, depending on such parameters as the length/diameter ratio of the chamber, and the vortex core contains essentially solid-body rotation.

The solution of the full Navier–Stokes equations for a rotating fluid is very difficult, and authors introduce simplifying assumptions in order to obtain a mathematical solution to the problem. Maslen & Moore (1956) obtained a solution for transverse (tangential) waves in a viscous heat-conducting but stagnant gas contained in an infinitely long circular cylinder. Sozou considered an inviscid compressible gas and investigated symmetrical-radial waves when the fluid is rotating as a Rankine vortex (1969*a*), and transverse waves in a fluid having uniform solid-body rotation (1969*b*) about the axis of its cylindrical container. Here we extend the latter work and investigate waves in a fluid rotating as a Rankine vortex about its axis. It is reported below that in the present flow régime there exists a further set of waves which we have termed 'slow waves'; also, under certain conditions, some waves break down and are unable to propagate. These phenomena are alien to the two flow régimes investigated previously.

2. Equations of the problem

We assume that our gas is contained in an infinitely long cylindrical cavity of radius d $(=ab;\ b \geqslant 1)$. We use a fixed polar co-ordinate system (R, θ, z) with the z-axis along the axis of symmetry of the cavity. The steady-state core of the gas is of radius a and rotates with constant angular velocity Ω about the z-axis. In the region $R > a$ we have potential flow and the angular velocity of the fluid is $a^2\Omega/R^2$. We also assume that our gas is perfect and the entropy is constant throughout the flow field, that is, we ignore gravity and assume that the pressure p and density ρ of the gas are connected by the relation

$$p = A\rho^{\gamma},$$

where A and γ are constants, γ being the ratio of the specific heats of the gas.

If we non-dimensionalize our quantities by

$$R = ar, \quad c_0(R) = c(r)c_0(0), \quad \rho_0(r) = \rho(r)\rho_0(0), \quad \Omega = \omega c_0(0)/a, \quad \mathbf{V}_0 = c_0(0)\mathbf{V},$$

where $\mathbf{V}_0$ is the fluid velocity, $c_0(R)$ is the speed of sound and $\rho_0(R)$ the gas density in the steady state, the integral of the momentum equation becomes

$$c^2 = \rho^{\gamma-1}\begin{cases} = \{\tfrac{1}{2}[(\gamma-1)\omega^2 r^2]\} + 1 & (0 \leqslant r \leqslant 1), \\ = (\gamma-1)\omega^2\left(1 - \dfrac{1}{2r^2}\right) + 1 & (1 \leqslant r \leqslant b), \end{cases} \tag{1}$$

and $\mathbf{V}$ is given by

$$\mathbf{V} = \begin{cases} (0, \omega r, 0) & (0 \leqslant r \leqslant 1), \\ (0, \omega/r, 0) & (1 \leqslant r \leqslant b). \end{cases} \tag{2}$$

We consider a two-dimensional perturbation $(\partial/\partial z = 0)$ of this state. The case of purely radial disturbances $(\partial/\partial\theta = 0)$ has been considered elsewhere (Sozou 1969*a*) and here we will be concerned with transverse waves. Thus, we let

$$\rho_1 = \rho_1'(r)\, e^{iK(\omega_2 t - \theta)},$$

and

$$\mathbf{V}_1 = (u, v, 0) = (u'(r), v'(r), 0)\, e^{iK(\omega_2 t - \theta)},$$

where the suffix 1 refers to the perturbation quantities, K is the order and ω_2 the angular velocity of the wave. The interface between the core and the potential annulus of the vortex is

$$r = 1 + \epsilon\, e^{iK(\omega_2 t - \theta)},$$

where ϵ is small.

If we now substitute the above relations in the continuity and the momentum equations making use of (2), eliminate the pressure by using the equation of state, and omit primes, to a first-order approximation, we obtain the following two sets of equations:

$$\left.\begin{aligned} &iK(\omega_2-\omega)\,\rho_1+\frac{1}{r}\left[\frac{d}{dr}(r\rho u)-iK\rho v\right] = 0, && (3a)\\ &iK(\omega_2-\omega)u-2\omega v+\frac{d}{dr}\left(\frac{c^2}{\rho}\rho_1\right) = 0, && (4a)\\ &iK(\omega_2-\omega)v+2\omega u-iKc^2\rho_1/\rho r = 0, && (5a)\end{aligned}\right\}\quad (0 \leqslant r \leqslant 1),$$

$$\left.\begin{aligned} &iK(r^2\omega_2-\omega)\,\rho_1+r\left[\frac{d}{dr}(r\rho u)-iK\rho v\right] = 0, && (3b)\\ &iK(r^2\omega_2-\omega)u-2\omega v+r^2\frac{d}{dr}\left(\frac{c^2\rho_1}{\rho}\right) = 0, && (4b)\\ &iK(r^2\omega_2-\omega)v-iKc^2r\rho_1/\rho = 0. && (5b)\end{aligned}\right\}\quad (1 \leqslant r \leqslant b).$$

Equations (4b) and (5b) show that the fluid velocity of the disturbance in the region $r \geqslant 1$—that is, in the region of potential flow—is derivable from a potential. This is due to the fact that the disturbance was assumed to be isentropic.

If we eliminate ρ_1 between (3) and (5) and between (4) and (5), and then eliminate v between the resulting pair of equations, we obtain two second-order linear differential equations in u. If we then use (1) and eliminate c and ρ these equations become

$$f_0(r)\frac{d^2u}{dr^2}+f_1(r)\frac{du}{dr}+f_2(r)u = 0 \quad (r \leqslant 1), \tag{6a}$$

$$g_0(r)\frac{d^2u}{dr^2}+g_1(r)\frac{du}{dr}+g_2(r)u = 0 \quad (b \geqslant r \geqslant 1), \tag{6b}$$

where

$$f_0 = r^2(a_0+a_1r^2+a_2r^4),\quad f_1(r) = r(b_0+b_1r^2+b_2r^4),$$
$$f_2 = c_0+c_1r^2+c_2r^4,\quad g_0 = r^2(d_0+d_1r^2+d_2r^4+d_3r^6),$$
$$g_1 = r(e_0+e_1r^2+e_2r^4+e_3r^6),\quad g_2 = h_0+h_1r^2+h_2r^4+h_3r^6+h_4r^8,$$

and

$$a_0 = 4(\omega_2-\omega),\quad a_1 = 4(\omega_2-\omega)\,[(\gamma-1)\omega^2-(\omega_2-\omega)^2],$$
$$a_2 = (\gamma-1)\omega^2(\omega_2-\omega)\,[(\gamma-1)\omega^2-2(\omega_2-\omega)^2],\quad b_0 = 12(\omega_2-\omega),$$
$$b_1 = 4(\omega_2-\omega)\,[(3\gamma-2)\omega^2-(\omega_2-\omega)^2],$$
$$b_2 = (3\gamma-1)\,(\omega_2-\omega)\omega^2[(\gamma-1)\omega^2-2(\omega_2-\omega)^2],\quad c_0 = 4(\omega_2-\omega)\,(1-K^2),$$
$$c_1 = 4(1-K^2)\,(\omega_2-\omega)\,[(\gamma-1)\omega^2-2(\omega_2-\omega)^2]+4\omega_2^2(3\omega_2-5\omega),$$

$$c_2 = [(\gamma-1)\omega^2 - 2(\omega_2-\omega)^2]\{(\omega_2-\omega)(1-K^2)[(\gamma-1)\omega^2-2(\omega_2-\omega)^2] + 2\omega_2^2(\omega_2-3\omega)\},$$

$$d_0 = (\gamma^2-1)\omega^4, \quad d_1 = -4\omega^2\{\gamma[(\gamma-1)\omega^2+1]+(\gamma-1)\omega\omega_2\},$$

$$d_2 = 4[(\gamma-1)\omega^2+1][1+(\gamma-1)\omega^2+2\omega\omega_2]+2(\gamma-1)\,\omega^2\omega_2^2,$$

$$d_3 = -4\omega_2^2[(\gamma-1)\omega^2+1],$$

$$e_0 = (3\gamma^2-2\gamma-5)\omega^4, \quad e_1 = 4\omega^3\omega_2(3-\gamma)-4\omega^2(3\gamma+1)[(\gamma-1)\omega^2+1],$$

$$e_2 = 12[(\gamma-1)\omega^2+1][(\gamma-1)\omega^2+2\omega\omega_2+1]-2(\gamma+1)\omega^2\omega_2^2,$$

$$e_3 = -4\omega_2^2[(\gamma-1)\omega^2+1],$$

$$h_0 = -[(\gamma+1)^2K^2-(\gamma^2-2\gamma-3)]\omega^4,$$

$$h_1 = 4K^2(\gamma+1)\omega^2[(\gamma-1)\omega^2+2\omega\omega_2+1]-4\omega^2\{[(\gamma-1)\omega^2+1](\gamma+3) + (3-\gamma)\omega\omega_2\},$$

$$h_2 = -4K^2\{[(\gamma-1)\omega^2+2\omega\omega_2+1]^2+(\gamma-1)\omega^2\omega_2^2\} + 4[(\gamma-1)\omega^2+1][(\gamma-1)\omega^2+2\omega\omega_2+1]+6(3-\gamma)\omega^2\omega_2^2,$$

$$h_3 = 8K^2\omega_2^2[(\gamma-1)\omega^2+2\omega\omega_2+1]+4\omega_2^2[(\gamma-1)\omega^2+1]$$

and

$$h_4 = -4K^2\omega_2^4.$$

Thus we have to solve (6*a*) in the region $0 \leqslant r \leqslant 1$, and (6*b*) in the region $1 \leqslant r \leqslant b$. The boundary conditions are:

$$u(0) \text{ finite}, \quad u(b) = 0,$$

and continuity of fluid velocity and density across $r = 1$; that is,

$$\Delta u = 0 \quad \text{and} \quad \frac{d}{dr}u(1+0) - \frac{d}{dr}u(1-0) = \frac{2u(1)\omega}{\omega_2-\omega}.$$

The last boundary condition is obtained from (3*a*), (5*a*), (3*b*) and (5*b*).

The expressions

$$c^2 - r^2(\omega_2-\omega)^2 \quad \text{and} \quad c^2r^2-(r^2\omega_2-\omega)^2$$

are factors of f_0 and g_0 respectively. Thus, f_0 and g_0 may have zeros in $0 \leqslant r \leqslant 1$ and $1 \leqslant r \leqslant b$, respectively. In order to investigate the behaviour of u at these zeros we note that (6*a*) and (6*b*) can be expressed in the form

$$\frac{d}{dx}\left(\frac{F(x)}{x}u'\right) = \frac{g(x)}{x^2}u, \tag{7}$$

where $x = r - r_0$, r_0 being the value of r at which f_0 or g_0 vanishes. $F(x)$ and $g(x)$ are functions, different for (6*a*) and (6*b*), which are regular and non-zero near the origin. The condition that (7) should have two regular solutions with finite derivatives at the origin is $$F(0)\,g'(0) = g^2(0).$$

On doing the arithmetic we find that F and g associated with (6*a*) and (6*b*) satisfy this condition at the respective zeros of f_0 and g_0, and therefore u and all its derivatives are finite at these zeros. But if these zeros occur at the interface—that is, if $c(1) = |\omega_2-\omega|$—the boundary condition expressing the continuity of density across the interface becomes

$$(\omega_2-\omega)[d^2u(1+0)/dr^2 - 2u(1)(c^4(1)+3\omega^2c^2(1)-2\omega^2)/c^4(1)]/(1+2\omega\omega_2-2\omega_2^2)$$
$$= (\omega_2-\omega)[d^2u(1-0)/dr^2+2u(1)(\omega^2-\omega_2^2c^2(1))/c^4(1)] - 2\omega\omega_2^2u(1)/c^2(1).$$

3. Method of computation

Equations ($6a$) and ($6b$) are solved by iteration as follows. For a specified ω, we guess an ω_2 and start from the origin for ($6a$), and from $r = b$ for ($6b$), satisfy the boundary conditions there, and proceed towards $r = 1$. Over the first five steps from the origin the solution is obtained by using the series expansion of u, and over the first five steps from $r = b$ the solution is obtained by using the Runge–Kutta method. Thence we build up the solution by using Hamming's predictor corrector method (cf. Ralston & Wilf 1961).

Since the solution involves only complementary functions, we choose $u^{K-1}(0) = (K-1)!$ for the Kth harmonic, multiply the solution obtained in the region $r \geqslant 1$ by an appropriate constant, and make u continuous. The remaining boundary condition at $r = 1$ is not satisfied and we use Newton's method for a new value of ω_2. This process is repeated, until the second boundary condition at $r = 1$ is satisfied to a high degree of approximation (inaccuracy $< 0{\cdot}0002$).

The computations were performed on the 1907 I.C.L. Computer of Sheffield University.

4. Results and discussion

We have taken γ as $1{\cdot}4$ and computed the first mode of the first two harmonics ($K = 1$ and 2) for several sets of data. Results of these computations are shown in figures 1–8 and in tables 1–3.

When the fluid is at rest, for a particular harmonic and mode, there are two transverse waves propagating in opposite directions with the same angular speed. When the fluid is rotating as a Rankine vortex about the axis of its cylindrical container the wave propagating in the direction of fluid rotation is speeded up. The amplitude of this wave, relative to its amplitude near the origin, increases with ω (see figures 1, 2). The boundary conditions show that there is a discontinuity in the first derivative of u at the interface. For this particular wave this derivative becomes larger on crossing the interface and increases with ω. Though ω_2 increases with ω, $d\omega_2/d\omega < 1$. Thus for some critical value of ω, say ω_c, ω_2 becomes equal to ω. When this stage is reached, $du(1+0)/dr$ and u in the region of potential flow become infinite.

It must be noted that when $\omega = \omega_c = \omega_2$, f_0 and f_1 vanish and ($6a$) becomes

$$f_2(r)u = 0$$

and the only plausible solution of this equation is $u = 0$. The difficulty is therefore partly due to the way in which we non-dimensionalized the amplitude of the disturbance. Thus, if we had set

$$u^{K-1}(0) = (\omega_2 - \omega)(K-1)!$$

the solution would tend to the correct limit, for $r < 1$, as ω tends to ω_c. However, as ω increases

$$(\omega_2 - \omega)u'(1+0)$$

also increases (for example when ω is 0, $0{\cdot}50$, 1 and $1{\cdot}25$ it is $0{\cdot}64$, $0{\cdot}70$, $5{\cdot}7$ and 64 respectively, for $K = 1$ and $b = 2$). Thus, it seems that as $\omega \to \omega_c$, this quantity tends to infinity, that is, on crossing the interface the wave again becomes vertical, and therefore very large in the region of potential flow, and the solution breaks down.

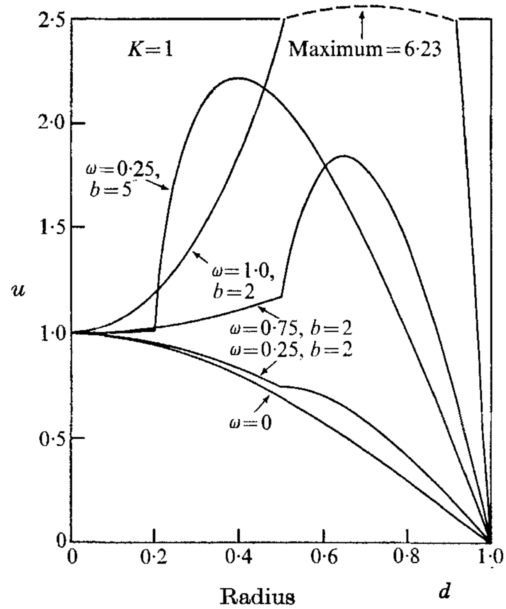

FIGURE 1. Amplitude of u (with $u(0) = 1$) as a function of the radial distance from the origin for the first-order harmonic wave propagating in the direction of fluid rotation, for various values of the parameters ω and b. The core radius is d/b.

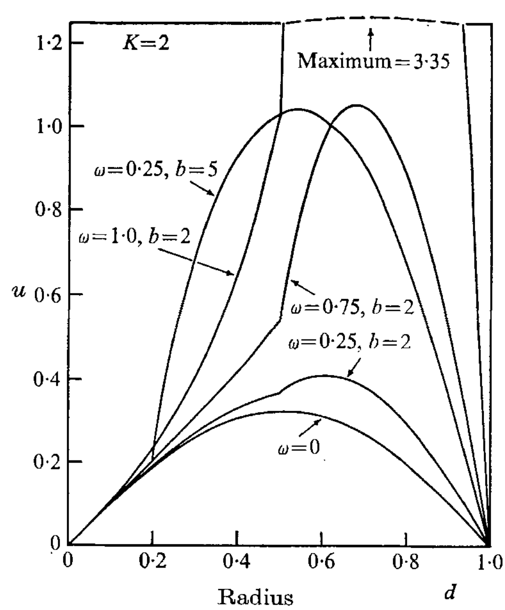

FIGURE 2. Amplitude of u (with $u'(0) = 1$) as a function of the radial distance from the origin for the second-order harmonic wave propagating in the direction of fluid rotation, for various values of the parameters ω and b. The core radius is d/b.

When $\omega \to \omega_c$ the assumption that the amplitude of the disturbance is small, which also implies small wave vorticity, is no longer valid and the linearized equations are no longer descriptive of the disturbed configuration. When $\omega = \omega_c$ the wave is in resonance with the frequency of the core of the rotating fluid, and this breakdown is possibly a resonance phenomenon. It is, however, significant that the wave cannot propagate in this particular mode when $\omega > \omega_c$, and this suggests that the refraction effects, caused by the velocity gradients, may be related to this breakdown.

In the case of uniform solid-body rotation (Sozou 1969*b*) and also in the case of radial (symmetrical) waves in Rankine vortex flow (Sozou 1969*a*) no breakdown of the flow régime occurs.

The numerical solution converges very rapidly when ω is not close to ω_c. As $\omega \to \omega_c$, and the amplitude of u becomes large, the convergence is very slow. Our computations indicate that when b, the ratio of the radius of the cylindrical container of the fluid to the radius of the core, is 2, 3 and 5, ω_c is about 1·45, 0·707 and 0·385 respectively when K is 1. When K is 2 the respective values of ω_c are about 1·36, 0·64 and 0·33. These points are indicated by circles on figure 5.

In comparing the wave frequencies with the various vortices it is worth recalling that, in dimensional units, the angular velocities of the wave Ω_2 and of the core of the rotating fluid Ω, are

$$\omega_2 c_0(0)/a = \omega_2 c_0(0) b/d \quad \text{and} \quad \omega c_0(0)/a = \omega c_0(0) b/d \tag{8}$$

respectively. Thus, in our vortex the angular velocity of the core is inversely proportional to its radius. For a given d, increasing b by a factor A is equivalent to speeding up the core of the vortex by the same factor and changing its radius by a factor of $1/A$.

For the data considered here $b\omega_c(b)\,(\sim \omega_c/a)$ is a decreasing function of b. If this is true for all b then ω_c tends to zero faster than a, and in the case of pure potential flow with an infinite vortex at the origin these waves cannot propagate in these modes.

Rotation depresses the amplitude of waves propagating opposite to the direction of fluid rotation, especially in the region of potential flow, as is quickly verified by inspection of figures 3 and 4 showing amplitudes of such waves.

The second boundary condition implies that, for these waves, du/dr decreases on crossing the interface. As is seen from figure 3, for a large potential flow annulus and large fluid angular velocities, the first-order harmonic waves tend to become vertical across the interface. However, these waves as well as the second-order harmonic waves (figure 4), exist for all the flow régimes investigated, and do not seem to break down.

Tables 1 and 2 show some of the computed values of ω_2 for various values of ω and b. Table 1 refers to the first ($K = 1$) and table 2 to the second ($K = 2$) harmonic wave.

Relative to the rotating core of the fluid, for a given vortex (ω and b), the waves propagating in the direction of fluid rotation are always slower than the waves propagating in the opposite direction, as can easily be verified from the data of tables 1 and 2.

Figure 5 shows the normalized wave angular velocity $\omega_2 b$ as a function of ω for various vortices shown in tables 1 and 2.

From figure 5 and tables 1 and 2 we deduce the following. For a given core angular velocity, the normalized wave angular velocity $\omega_2 b$ is maximum in the

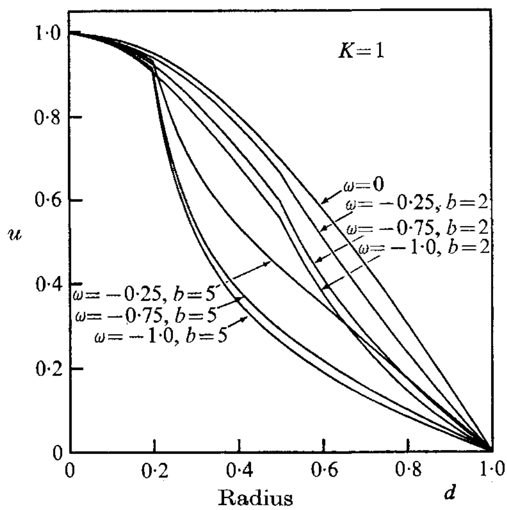

FIGURE 3. Amplitude of u (with $u(0) = 1$) as a function of the radial distance from the origin for the first-order harmonic wave propagating opposite to the direction of fluid rotation for various values of the parameters ω and b. The core radius is d/b.

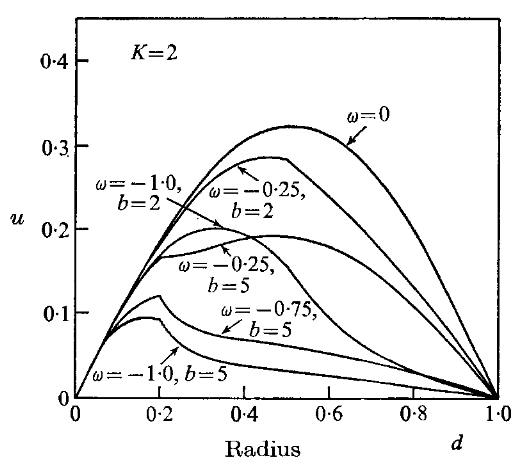

FIGURE 4. Amplitude of u (with $u'(0) = 1$) as a function of the radial distance from the origin for the second-order harmonic wave propagating opposite to the direction of fluid rotation for various values of the parameters ω and b. The core radius is d/b.

case of solid body rotation (for any ωb constant, $\omega_2 b$ is maximum when b is 1, see tables 1 and 2) in agreement with the case of symmetrical waves (Sozou 1969a).

For waves propagating opposite to the direction of fluid rotation (ω negative) $\omega_2 b$ decreases for small values of ω. In the case of the first-order harmonic wave

$\omega_2 b$ quickly reaches a minimum, and thence, as the fluid is speeded up, it increases, and for large fluid velocities these waves, which are slower for solid-body rotation (see the broken curves of figure 5), are much faster than in the absence of fluid rotation. For second-order harmonic waves, and the range of

ω	$b = 1$	$b = 2$	$b = 3$	$b = 5$	$b = 10$
−2·00	2·5562	1·7256	1·1191	0·6303	
−1·50	2·2234	1·3942	0·9209	0·5297	
−1·00	1·9852	1·1277	0·7544	0·4444	0·2187
−0·50	1·8428	0·9595	0·6439	0·3861	0·1928
−0·25	1·8221	0·9228	0·6198	0·3715	0·1860
−0·10	1·8267	0·9167	0·6126	0·3681	0·1843
0	1·8412	0·9206	0·6137	0·3682	0·1841
0·10	1·8608	0·9297	0·6184	0·3702	0·1848
0·25	1·9050	0·9534	0·6314	0·3765	—
0·50	2·0159	1·0177	0·6688	—	—
1·00	2·3750	1·2177	—	—	—
1·25	2·6123	1·3414	—	—	—

TABLE 1. Values of ω_2 for $K = 1$

ω	$b = 1$	$b = 2$	$b = 3$	$b = 5$	$b = 10$
−2·00	0·7477	0·3492	0·3277	0·2971	
−1·50	0·8746	0·4132	0·3525	0·2861	
−1·00	1·0390	0·4996	0·3865	0·2789	
−0·50	1·2518	0·6146	0·4360	0·2827	
−0·25	1·3804	0·6845	0·4621	0·2913	
−0·10	1·4662	0·7308	0·4922	0·2990	0·1512
0	1·5272	0·7636	0·5090	0·3054	0·1527
0·10	1·5912	0·7978	0·5270	0·3130	
0·25	1·6937	0·8520	0·5562	0·3253	—
0·50	1·8826	0·9504	0·6106	—	—
1·00	2·3307	1·1770	—	—	—
1·25	2·5876	1·3041	—	—	—

TABLE 2. Values of ω_2 for $K = 2$

angular velocities considered here, if b is not very large, $\omega_2 b$ decreases monotonically as ω increases. However, for large potential region vortices—for example, when b is 5—$\omega_2 b$ reaches a minimum, and thence it increases with ω.

For a given fluid velocity at the core boundary—that is, for a given ω, as the size of the core decreases and the region of potential flow increases (from zero)—the wave angular velocity, when K is 1, increases until it reaches a maximum, depending on ω, and thence it decreases with the size of the core. The second-order harmonic waves exhibit the same behaviour for positive ω and precisely the opposite behaviour for negative ω.

If account is taken of the dependence of the temperature at the centre of the cavity, and thus of $c_0(0)$ on rotation, the above interpretation of our results may need some modifications, since Ω and Ω_2 are proportional to $c_0(0)$.

Besides the waves discussed above there is another train of waves propagating in the direction of fluid rotation. These waves lag behind the rotating core of the fluid and are termed 'slow waves' in order to be distinguished from the waves rotating faster than the core, in the same direction. Since $\omega > \omega_2$, the second boundary condition implies that the amplitude of these waves decreases on crossing the interface, and our computations show that it decreases monatomically from the interface to the boundary. Amplitudes of these waves, for various parameters, are shown in figures 6 and 7 for the first and second harmonic waves, respectively.

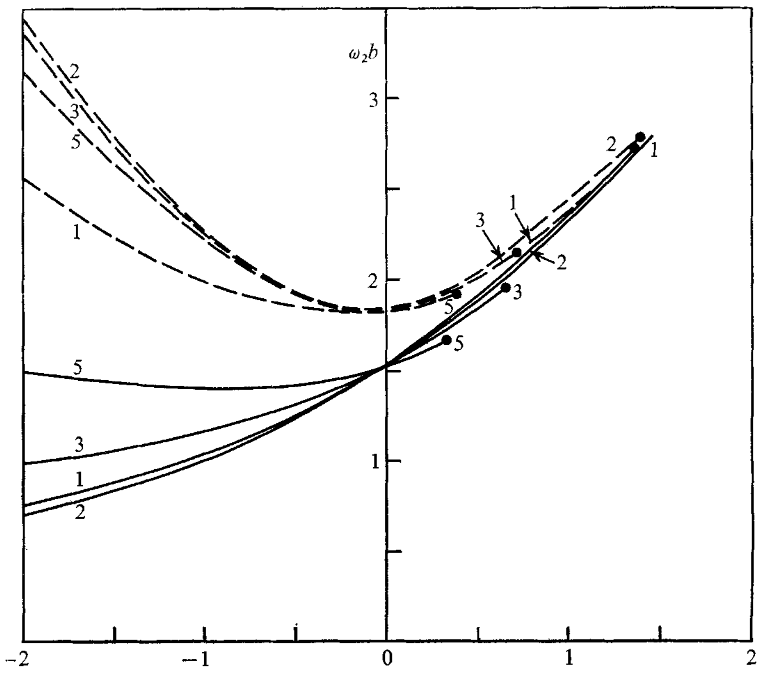

FIGURE 5. Normalized wave angular velocity $\omega_2 b$ as a function of ω. The broken and solid curves refer to the first and second harmonic ($K = 1$, $K = 2$), respectively. 1, 2, 3 and 5 refer to the cases when b is 1, 2, 3 and 5 respectively. For positive ω, curve '3' is very close to '1'.

For all the parameters investigated, most of which are shown in table 3, the first-order slow harmonic waves exist. The second-order slow harmonic waves exist when the potential annulus is not very large. As ω increases, the amplitude of these waves, mainly in the potential flow region, becomes depressed. For a vortex having a sufficiently large potential annulus and an appropriate core angular velocity the amplitude of these waves changes sign in the potential flow region; that is, these waves cannot propagate in this particular mode; for example, when b is 5 the second-order slow harmonic wave breaks down for a value of ω between 0·4 and 0·5.

As the potential annulus of the flow régime decreases, the wave velocity increases and approaches the angular velocity of the core. In the limit, of no potential annulus, the two angular velocities are equal and the amplitude of the

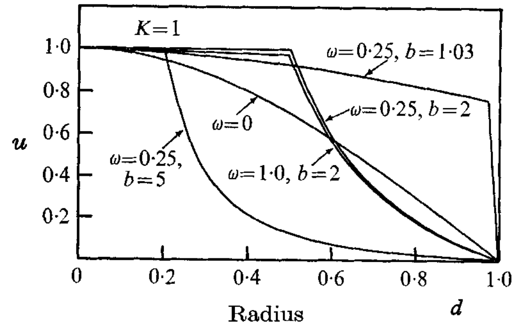

FIGURE 6. Amplitude of u (with $u(0) = 1$) as a function of the radial distance from the origin, for the first-order slow harmonic wave, for various values of the parameters ω and b. The core radius is d/b.

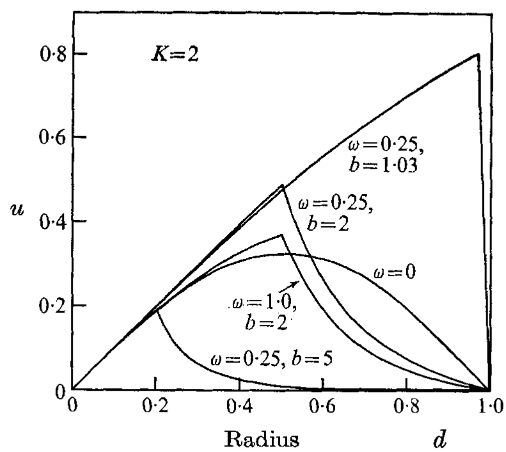

FIGURE 7. Amplitude of u (with $u'(0) = 1$) as a function of the radial distance from the origin, for the second-order slow harmonic wave, for various parameters of ω and b. The core radius is d/b.

ω	b	$K = 1$, ω_2	$K = 2$, ω_2	b	$K = 1$, ω_2	$K = 2$, ω_2
2	5	0·0769	—	2	0·4519	0·8719
1·5	5	0·0582	—	2	0·3454	0·6948
1·0	5	0·0392	—	2	0·2367	0·4941
0·75	5	0·0296	—	2	0·1807	0·3814
0·50	5	0·0199	—	2	0·1222	0·2603
0·25	5	0·0100	0·1246	2	0·0622	0·1321
0·25	1·5	0·1105	0·1490	1·2	0·1729	0·1848
0·25	1·09	0·2099	0·2132	1·03	0·2353	0·2359
0·10	5	0·0040	0·0050	2	0·0250	0·0531
0·10	1·5	0·0444	0·0598	1·2	0·0694	0·0741
0·10	1·09	0·0841	0·0854	1·03	0·0942	0·0944

TABLE 3. Slow waves.

wave is zero. Thus these waves are a special feature of the Rankine vortices, and do not exist in the case of pure solid-body rotation. Due to the manner of non-dimensionalization of our quantities, it is not shown in figures 6 and 7 that the amplitude of these waves tends to zero as b tends to 1. However, as shown for the fast waves, as ω_2 tends to ω, by the appropriate non-dimensionalization, u tends to its correct limit zero for $r \leqslant 1$; that is, as b tends to 1, the maximum amplitude of these curves, $u(1)$, tends to zero.

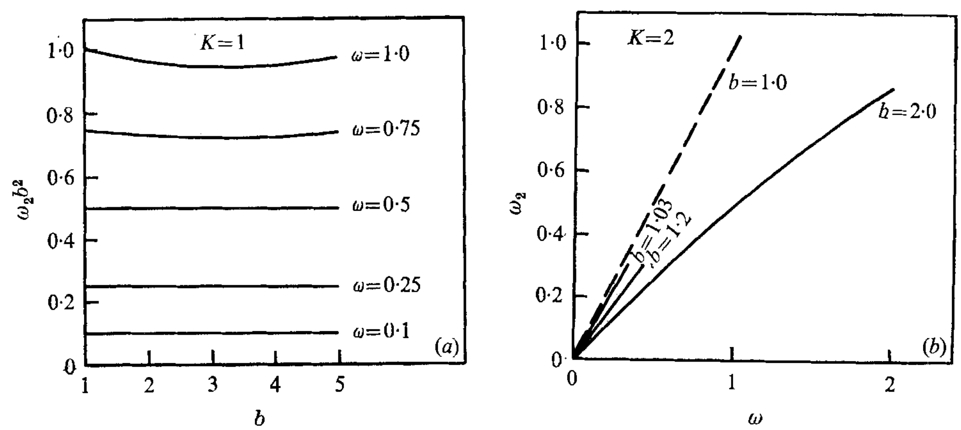

FIGURE 8. (a) $\omega_2 b^2$ as a function of b for the first-order slow harmonic wave. (b) ω_2 as a function of ω for the second-order slow harmonic wave for various values of the parameter b.

Mathematically the frequency of the slow waves is the manifestation, due to rotation, of the first zero (the trivial case $\omega_2 = 0$) of the Bessel functions of integral order greater than 0, which provide solutions of our problem, when ω is zero.

The angular velocity of the first-order slow harmonic waves, for $\omega \leqslant 0{\cdot}5$, fits very well into the formula

$$\omega_2 = \omega/b^2 \sim \omega a^2, \tag{9}$$

i.e. ω_2 is proportional to the total angular velocity of the core. For larger values of ω and moderate values of b this formula is only approximately correct; for example, when ω is 2, the computed value of ω_2 corresponding to $b = 2$ and 5 is less than that given by the above formula by about 9·5 and 4%, respectively.

For the range of angular velocities considered here the ω_2 corresponding to the second-order harmonic wave is very nearly proportional to ω for $\omega \leqslant 0{\cdot}5$, though the constant of proportionality depends on b. For larger ω, $d\omega_2/d\omega$ is a slowly decreasing function of ω, as can be seen by inspection of table 3 or figure 8(b).

5. Applications

Our results concerning slow waves are in excellent agreement with experimental observations of sound generated by the escape of a vortex from the open end of a tube, known as the vortex whistle. Experiments carried out by

Vonnegut (1954) show that when the fluid leaves the tube in which it is rotating, the vortex becomes unstable and whips around at an angular velocity about the same as its rotational velocity. The sound emitted has the precession frequency of the unstable vortical motion. Our results suggest that this is due to the fact that the periphery of the escaping fluid, by coming into contact with the open air, acquires an angular velocity different from that of the core, thus enabling the slow waves to propagate. The flow régime is almost entirely core and the fluid and wave angular velocities are equal, in agreement with our results.

Detailed experiments carried out by Chanaud (1963) show that the sound field of the vortex whistle is that of the first harmonic and corresponds to a rotating dipole in the plane of the tube exit. Figure 6 shows that the particle velocity (and hence displacement) of the core associated with the first-order slow harmonic wave is almost constant with radius. It therefore follows that the sound field associated with this wave corresponds to a rotating dipole.

Chanaud's experiments with a water vortex showed that when the core almost filled the whistle tube, the frequency of the whistle was within 10% of the rotational speed of the core, again in reasonable agreement with our theory (figure 8, table 3). By varying the vortex tube length L and thus the thickness δ of the boundary layer, which may be interpreted as our potential annulus, Chanaud found that the decrease in the whistle frequency was larger than the decrease in the average fluid angular velocity. Our theory suggests that this discrepancy is due to the fact that the wave frequency of the first harmonic is proportional to the total angular velocity of the core (see (9) of §4), and not of the whole fluid. Simple arithmetic shows that the predictions of our theory are in very good agreement with these experimental observations. If we let $R(d_1)$ denote the Reynolds number based on the tube diameter d_1, and assume that the boundary layer was turbulent ($R(d_1)$ was 4950), with

$$\delta \sim L^{\frac{4}{5}}\left(\frac{d_1}{R(d_1)}\right)^{\frac{1}{5}},$$

then

$$b \mathrel{\dot{\approx}} 1/(1-2\delta/d_1).$$

On using (9) we obtain

$$\omega_2/(\omega_2)_0 = 1/b^2 = \left[1-K'\left(\frac{L}{d_1}\right)^{\frac{4}{5}}\right]^2,$$

where the subscript zero refers to $L = 0$.

In figure 9 we compare theory and experiment, with K' being evaluated from Chanaud's results when L/d_1 is 10.

It appears that ours is the first theoretical prediction of the slow waves and their association with the vortex whistle.

Recently Gyarmathy (1968) made optical measurements for a high-speed gaseous vortex rotating in a tube very much like our Rankine vortex. His 'b' was 7·26. Gyarmathy inferred from his measurements that the core was rotating at one million revolutions per minute and the fluid velocity at the periphery of the core was 1·6 times the local speed of sound. Two distinct density fluctuations were observed. A fast fluctuation having a frequency of the order of 10^4 c/s and regular sine structure and an irregular relatively slow fluctuation lying roughly in the region of 300–500 c/s. This slow fluctuation is absent at large distance from the axis. For this vortex our first-order slow harmonic wave has a frequency 317 c/s. Gyarmathy's data would make our $\omega \pm 1{\cdot}6$ and give a first-order 'fast' wave propagating opposite to the direction of fluid rotation with a frequency 5000 c/s.

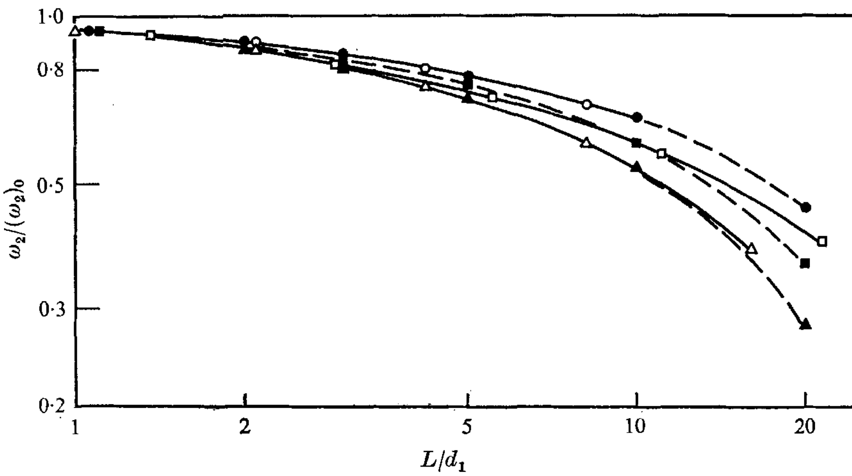

FIGURE 9. Our slow-wave frequencies for the first harmonic (broken curves) and Chanaud's experimental results for a water-vortex whistle (reproduced with the kind permission of the *J. Acoust. Soc. America*). The curves have been matched where L is $10d_1$. – – –, theory. Chanaud: ○, $d_1 = 0{\cdot}225$ in.; □, $d_1 = 0{\cdot}449$ in.; △, $d_1 = 0{\cdot}652$ in.

To our knowledge, there is very little experimental data on acoustic waves in vortices. Direct experimental evidence of the fast-wave breakdown is not yet available. Indirect evidence is provided by the fact whilst several cases of waves travelling opposite to the direction of fluid rotation have been recorded (Swithenbank 1965), it appears that there are no examples of waves travelling in the direction of fluid rotation.

Evidence for the quantitative effect of ω on the wave velocity is also sparse and the main source is studies of oscillatory combustion in solid propellant rocket motors. Swithenbank & Sotter (1964) in their experiments in connexion with solid propellant rocket instability observed the first-order (first mode) harmonic wave going opposite to the direction of fluid rotation. The fluid velocity at the edge of the core, which had a diameter $\sim 0{\cdot}75$ in., was approximately equal to the local speed of sound; that is, $\omega \sim -1$ and $c_0(0)$ was about 3200 ft./sec. The diameter of the tube was ~ 4 in., though the flow régime outside the core, due to viscous dissipation was not quite potential. This would make our $b \sim 5{\cdot}3$ and $\omega_2 \sim 0{\cdot}41$, where ω_2 is extrapolated from table 1, and give a wave frequency $\sim 6{\cdot}7$ kc/s. The observed oscillation frequency varied between 5 and 10 kc/s.

Other workers studying a comparable system (Angelus 1960, p. 527; Brownlee & Marble 1960, p. 455) report that the observed frequencies of the transverse waves are in general agreement with the value obtained from simple acoustic theory without fluid rotation. If we assume, as will most probably be the case in practice, that the total temperature at the edge of the core will be approximately the same as when the fluid is stagnant, we will have

$$c_0(0)_\omega = c_0(0)_0/[1+(\gamma-1)\omega^2/2]^{\frac{1}{2}} \sim 0{\cdot}9c_0(0)_0$$

when $\omega \sim \pm 1$, where $c_0(0)_x$ denotes the value of $c_0(0)$ when ω is x. Thus, for comparison with the frequencies corresponding to stagnant gas we must multiply our $\omega_2(\omega)$ by a factor $1/[1+(\gamma-1)\omega^2/2]^{\frac{1}{2}}$. When ω is ~ -1 this would make the frequencies of the first harmonic predicted by the theory about 8% higher than the frequencies corresponding to the case when the gas is stationary. The experimental results could be in error by up to 10% and thus our theory is also in general agreement with these observations.

Our investigations have shown that whilst available experimental results are in broad agreement with the theory of the fast wave presented here, further experiments are required to verify the theory in detail.

REFERENCES

Angelus, T. A. 1960 *Solid Propellant Rocket Research*, vol. 1. New York: Academic.

Brownlee, W. G. & Marble, F. E. 1960 *Solid Propellant Rocket Research*, vol. 1. New York: Academic.

Cantrell, R. H. & Hart, R. W. 1964 *J. Acoust. Soc. Am.* **36**, 697.

Chanaud, R. C. 1963 *J. Acoust. Soc. Am.* **35**, 953.

Gyarmathy, G. 1968 *A.I.A.A. Fluid and Plasma Dynamics Conference*, paper no. 68–694.

Keyes, J. J. 1960 *Proceedings of the* 1960 *Heat Transfer and Fluid Mechanics Institute, Stanford.*

Lighthill, M. J. 1966 *J. Fluid Mech.* **26**, 411.

Maslen, S. H. & Moore, F. K. 1956 *J. Aero. Sci.* **23**, 583.

Ralston, A. & Wilf, H. S. 1961 *Mathematical Methods for Digital Computers*, part III (8). New York: Wiley.

Roschke, E. J. & Pivirotto, J. J. 1965 *Jet Propulsion Lab. Tech. Report*, no. 32–789.

Sozou, C. 1969*a* *J. Acoust. Soc. Am.* (To be published.)

Sozou, C. 1969*b* *J. Fluid Mech.* **36**, 605.

Swithenbank, J. 1965 *2nd Interagency Chemical Rocket Propulsion Group Meeting, Los Angeles.*

Swithenbank, J. & Sotter, G. 1964 *A.I.A.A. J.* **2**, 1297.

Vonnegut, B. 1954 *J. Acoust. Soc. Am.* **26**, 18.